ELSEVIER

Thermochimica Acta 304/305 (1997) 267–275

thermochimica acta

Phase angle correction for TMDSC in the glass-transition region

S. Weyer, A. Hensel, C. Schick*

University of Rostock, Department of Physics, Universitätsplatz 3, 18051 Rostock, Germany

Received 14 December 1996; accepted 14 March 1997

Abstract

Temperature-modulated DSC (TMDSC) allows the determination of frequency (time) dependent heat capacities. If heat capacity is frequency dependent, for example, in the glass-transition region, one get a phase angle between heating rate and heat-flow rate which is related to material intrinsic properties. Because heat does not propagate but flows, the time-consuming heat transfer into the sample yields an additional phase angle. This phase angle has to be taken into account if one wants to calculate the imaginary part of the complex heat capacity of the sample from the measured phase angle. The heat transfer related phase angle depends on frequency, heat capacity and heat conductance. In the case of glass-transition, heat capacity and heat conductance may change in the respective temperature interval. A correction for the corresponding phase angle is suggested. © 1997 Elsevier Science B.V.

Keywords: Complex heat capacity; Glass transition; Phase angle; Temperature-modulated DSC (TMDSC)

1. Introduction

The glass transition is at present a central problem of condensed matter physics, for which no generally accepted theory exists. There are two different aspects of glass transition:

- vitrification or thermal glass transition
- dynamic glass transition (relaxation process)

Vitrification means the change from the liquid (equilibrium) to the solid (glassy, non-equilibrium) state without structural changes. The dynamic glass transition is related to the corresponding relaxation process in the liquid state.

With temperature-modulated differential scanning calorimetry (TMDSC) both aspects of glass transition can be observed simultaneously. Additional information about glass transition is available from such measurements as well as the opportunity to check different models of glass transition in more detail, see Refs. [1,2]. The thermal glass transition is visible in the underlying signal, related to the underlying heating or cooling rate. Therefore, the underlying rate determines the time scale in respect to the thermal glass transition. With the temperature modulation the dynamic glass transition can also be observed. The corresponding time scale is given by the modulation period (frequency). From the heat-flow rate response to temperature modulation a complex heat capacity may be derived. In a relaxation region, for example, in the glass-transition region, a step in the real part and a peak in the imaginary part of complex heat capacity occurs. The latter is related to a phase angle change between heating rate and

*Corresponding author.

0040-6031/97/$17.00 © 1997 Elsevier Science B.V. All rights reserved
PII S0040-6031(97)00180-9

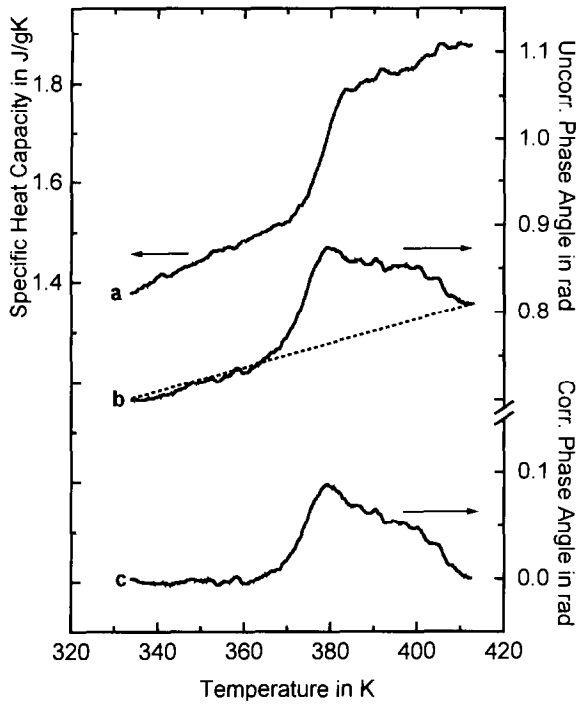

Fig. 1. TMDSC measurement of a polystyrene-granulate; a – modulus of complex heat capacity; b – uncorrected phase angle between heat-flow rate and heating rate; c – corrected phase angle according to the correction supposed by Perkin–Elmer and TA Instruments using the dotted line. (PE DDSC-7: $m_{PS} = 9.16$ mg; $t_p = 1$ min; $q_0 = -0.5$ K/min; $T_a = 0.2$ K.)

heat-flow rate which depends on material intrinsic parameters.

As heat does not propagate but flows, the time-consuming heat transfer into the sample needs time and yields a phase shift between heating rate and heat-flow rate signal. This unavoidable phase angle has to be taken into account if one wants to calculate the imaginary part of complex heat capacity from measured phase angles. Correction for this part of the measured phase angle is often realised in the today's TMDSC software by subtracting a linear interpolated line between starting and end point of the phase angle curve, see Fig. 1 dotted line. In the case of non-optimal measuring conditions such a correction yields unrealistic results for the phase angle and therefore for the imaginary part of complex heat capacity, see Fig. 1 Curve c.

It seems to be necessary to choose proper measurement conditions and to derive a better correction to obtain the true phase angle due to the intrinsic process of the sample. Therefore, the influence of different quantities on heat transfer related phase angle are studied and recommendations for optimal measurement conditions are given. But, if one wants to cover the whole frequency range available with TMDSC, it is also necessary to extract the correct phase angle information from measurements got under non-optimal conditions. Especially at higher frequencies around 0.1 Hz it is not possible to get undisturbed phase angle information with the today's TMDSC apparatus. The aim of this paper is to suppose a better correction for this heat flow related phase angle in the glass-transition region to be able to cover the whole available frequency range of TMDSC.

2. Background of TMDSC operation

Temperature-modulated DSC (TMDSC) [3–5] is an extension to standard DSC. The linear heating or cooling rate as normally used in DSC is superimposed with a periodical temperature oscillation

$$T(t) = T_0 + q_0 t + \sum_{n=1}^{\infty} (T_{a_n} \sin(n\omega t)) \tag{1}$$

where T_0 is the initial temperature, q_0 the constant underlying heating or cooling rate which in the following is generally referred to as heating rate, T_{a_n} the temperature modulation amplitude of the nth-harmonic and $\omega = 2\pi/t_p$ the angular frequency with t_p the modulation period.

Dependent on the ratio between the amplitudes T_{a_n} the curve shape may be different, for example, $T_{a_1} \neq 0$ and all other $T_{a_n} = 0$ yields a sinusoidal and $T_{a_1} : T_{a_3} : T_{a_5} : \ldots : T_{a_{2n-1}} = 1 : -1/9 : 1/25 : \ldots : (-1)^{n+1} * 1/(2n-1)^2$ in saw-toothlike modulation. From Eq. (1) the oscillating heating rate $q = dT/dt$ follows

$$q(t) = q_0 + \sum_{n=1}^{\infty} (n\omega T_{a_n} \cos(n\omega t)) \tag{2}$$

with heating rate modulation amplitude for the nth-harmonic $q_{a_n} = n\omega T_{a_n}$. Because of this time dependent heating rate a modulated heat-flow rate containing the response to the underlying heating rate q_0 and to the oscillation part with the same harmonics as in the

temperature signal according to

$$\Phi(t) = \Phi_{\text{total}} + \sum_{n=1}^{\infty}(\Phi_{a_n}\cos(n\omega t - \delta_n) \tag{3}$$

can be observed. From this measured heat-flow rate different quantities can be determined. Gliding average of the heat-flow rate over one period yields the so-called total heat-flow rate, $\Phi_{\text{total}} = q_0 C_{\text{p total}}$, comparable with that of a standard DSC measurement at the same heating rate q_0 [4,6,7]. Subtracting this averaged heat-flow rate from the measured one results in the oscillation part, the dynamic component. From this dynamic component the amplitude Φ_{a_1} of the first harmonic and the phase angle δ between heat-flow rate and heating rate can be determined by Fourier analysis. Other quantities can be calculated from this amplitude and phase angle as pointed out by Reading, Wunderlich and Schawe [3–8]. In the following, we focus on the complex heat capacity and its imaginary part [6,8].

At first an in-phase and an out-of-phase component of the heat-flow rate can be determined according to

$$\Phi_{\text{in}}(t) = \frac{2}{t_p}\int_{t-t_p/2}^{t+t_p/2}\Phi(t')\cos(\omega t')\mathrm{d}t' \tag{4}$$

and

$$\Phi_{\text{out}}(t) = \frac{2}{t_p}\int_{t-t_p/2}^{t+t_p/2}\Phi(t')\sin(\omega t')\mathrm{d}t' \tag{5}$$

From this the heat-flow rate amplitude

$$\Phi_a = \sqrt{\Phi_{\text{in}}^2 + \Phi_{\text{out}}^2} \tag{6}$$

and the phase angle

$$\delta = \arctan\left(\frac{\Phi_{\text{out}}}{\Phi_{\text{in}}}\right) \tag{7}$$

can be determined. If the time scale is chosen in such a way that the phase angle of the heating rate equals zero, then δ equals the phase angle between heat-flow rate and heating rate.

The reason for a non-zero phase angle δ in the heat-flow rate signal of TMDSC experiments may be different. One part of δ is due to the heat transfer in the sample [4]. This part δ_{ht} is strongly dependent on the thermal contact between sample and thermometer and on the heat conductance of the sample itself. This effect is well known from AC calorimetry and used to check for proper measuring conditions, see [9] and references therein. Solving the differential equations for heat transfer [7,10,11] yields for small phase angles

$$\delta_{\text{ht}} = \frac{\omega C_p}{K} \tag{8}$$

with K heat conductance of the heat-flow path between sample and thermometer.

The resulting phase angle depends on the heat-flow rate which is related to the heat capacity of the sample as well as the sample support and shows big effects, for example, at first-order phase transitions as well known from AC calorimetry [12] which can be detected in TMDSC too [13].

In the case of relaxation processes, like glass transition, an additional phase angle δ_s caused by the relaxation process can be observed [8]. This phase angle δ_s is related to sample properties and not to heat transport processes.

As pointed out by different authors in this issue, the heat capacity can be considered to be a complex quantity [9,14–17].

$$C_p^* = C_p' - iC_p'' \tag{9}$$

The modulus $|C_p^*|$ can be obtained from

$$|C_p^*| = \frac{\Phi_a}{q_a} \tag{10}$$

with q_a heating rate amplitude. Real part C_p' and imaginary part C_p'' are given by

$$C_p' = |C_p^*|\cos\delta_s \tag{11}$$

$$C_p'' = |C_p^*|\sin\delta_s, \tag{12}$$

where C_p^* and δ_s are functions of temperature and frequency. The phase angle δ_s means the phase angle caused by the relaxation processes in the sample, it is not the one measured between heat-flow rate and heating rate, given by Eq. (7), which includes phase angle due to heat transfer processes too. Therefore, estimation of the sample caused phase angle δ_s is one of the central problems of complex heat capacity determination in TMDSC.

3. Experimental

The TMDSC experiments were performed with Perkin–Elmer DDSC-7 and Setaram DSC-121, both in standard (DSC) as well as in temperature-modulated (TMDSC) mode.

The temperature scale of the calorimeter was calibrated in the common way with indium and lead [18] and checked in the TMDSC mode with the smectic A to nematic transition of M 24 [13]. The heat-flow rate calibration was done with sapphire in the DSC mode. The purge gas was nitrogen at a flow rate of 1 l/h. The temperature of the calorimeter block of the Perkin–Elmer DSC-7 and the room temperature were kept well stabilised at (-75 ± 0.1) and (27 ± 0.5)°C, respectively, in order to realise reproducible scans. Sample mass was of about 10 and 100 mg for the DSC-7 and DSC-121, respectively. TMDSC experiments were performed with saw-tooth modulation using the Perkin–Elmer DDSC software or by setting up the respective temperature program with the standard programming module from Setaram. Unless otherwise stated the following modulation parameters were used: Underlying cooling rate $q_0 = 0.5$ K/min; temperature amplitude $T_a = 0.2$ K, modulation period $t_p = 1$ min. To study the glass transition near thermal equilibrium quasi-isothermal measurements were performed with the Setaram DSC 121. Then the modulation amplitude was 0.1 K and the modulation period in the range 5 to 100 min. To start from an equilibrium state of the sample and to be independent from thermal history all measurements were performed on cooling. The quasi-isothermal measurements also starts at the highest temperature followed by a stepwise decreasing of temperature. From the dynamic part of the heat-flow rate the modulus of complex heat capacity $|C_p^*|$ and the phase angle δ (according to (6) and (7), respectively) were determined using the same self made evaluation software for both calorimeters. The result is the same as from the built in Perkin–Elmer DDSC software but without baseline subtraction and any correction of the measured phase angle.

Fig. 1 shows results for $|C_p^*|$ and δ in the glass transition range of polystyrene (PS 168N from BASF). To demonstrate the problems in phase angle determination in TMDSC, a sample with bad thermal contact was used. According to Kramers–Kronig relation [19] the step like increase in the real part of C_p' (which is nearly equal to $|C_p^*|$) implies a peak in the imaginary part C_p'' and the phase angle δ_s. In other words, the imaginary part and the phase angle δ_s should disappear outside the relaxation region. This is well known from other relaxation processes, for example, dielectric or dynamic mechanical relaxation. In Fig. 1 Curve a the step in $|C_p^*|$ can be observed but in Curve b a peak in the phase angle is not visible. The non-zero value of the phase angle over the whole temperature range can not be related to the glass relaxation process but to the heat transfer. To correct for this phase angle the today's software's offered by Perkin–Elmer and TA Instruments subtracts a straight line between the starting and the end point of the phase angle curve, see Fig. 1 dotted line. The result of such a correction is shown in Fig. 1 Curve c. This type of correction yields an unrealistic broad and non-symmetric peak in δ which differs considerably from the expected shape.

As the measured phase angle δ is the superposition of that due to heat transfer δ_{ht} and that of a relaxation processes in the sample δ_s, we may study the phase angle due to heat transfer separately. The aim of this study was to find optimal measuring conditions and a method for more realistic phase angle correction. According to Eq. (8) we tried to vary frequency, heat capacity and heat conductance independent of each other to study their influence on the measured phase angle in the glass-transition region of PS.

4. Results and discussion

To study the influence of sample heat capacity on the measured phase angle, two planar samples with different thicknesses and therefore different masses and heat capacities were prepared, see Fig. 2 Curve a and b. As can be seen the phase angle of Sample b does not equal twice that of Sample a as should be the case, see Eq. (8). This is because the thermometer is not in direct contact with the sample. Consequently the phase angle due to heat transfer inside the oven and the pan as well as that caused by the unsymmetry of the ovens must be considered too. It should be possible to determine this part of the phase angle by an empty pan measurement. We have tried to do this. But, as the differential signal for the empty pan measurement is very small the heat-flow rate curve is dominated by the peaks at the points of switching from cooling to

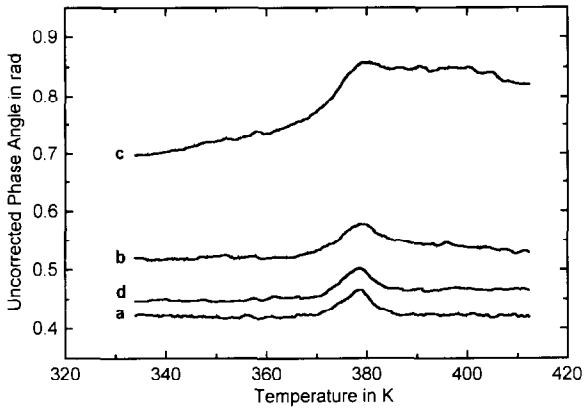

Fig. 2. Uncorrected phase angles between heat-flow rate and heating rate of TMDSC measurements of different polystyrene samples in the glass transition region; a – thin disk, m_{PS} = 12.67 mg; b – thick disk, m_{PS} = 27.23 mg; c – granulate, m_{PS} = 9.16 mg; d – thick disk with silicon oil, m_{PS} = 27.23 mg. (PE DDSC-7: t_p = 1 min; q_0 = −0.5 K/min; T_a = 0.2 K.)

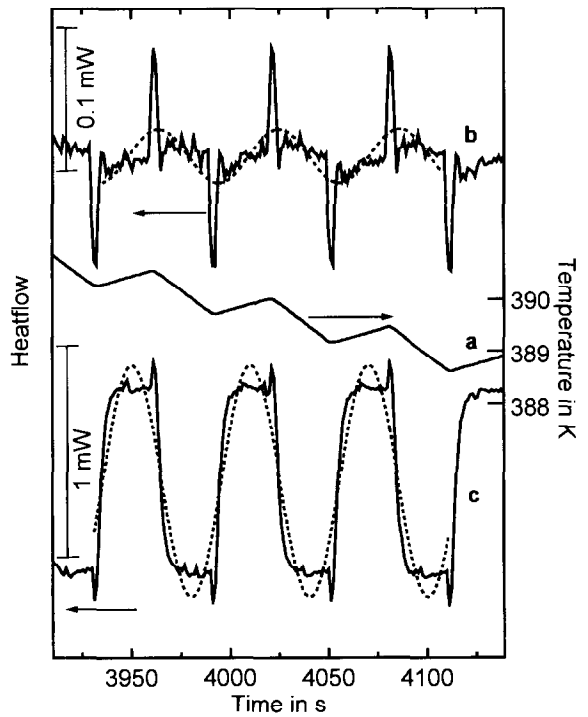

Fig. 3. Temperature program (a) and heat-flow rates for an empty pan (b) and for the thin disk (c). The dotted lines indicate the calculated first harmonics.

heating and vice versa, see Fig. 3 Curve b. Such peaks are well known from standard DSC measurements at the beginning and the end of a scan. The Fourier analysis of a curve with such artefacts results in a meaningless amplitude (to big) and phase angle (about $\pi/2$), see Fig. 3 Curve b dotted line. It is, however, not possible to determine the phase angle caused by the heat transfer inside the oven from such measurements with saw tooth modulation. This point is important in any case where these peaks appear and the results of Fourier analysis are influenced. As an example in Fig. 3 Curve c the measured heat-flow rate for the smallest sample used in this study is presented. The peaks are visible but do not dominate the calculated first harmonic (dotted line). When heat capacity is decreasing during an experiment the influence of these peaks may increase and result in an artefact of an additional phase angle shift.

From Fig. 1 Curve b no single peak in the phase angle but a superposition of a peak and a step can be observed. The reason for this step may be the heat capacity change ΔC_p at the glass transition which induces a phase angle change $\Delta\delta$ according to Eq. (8)

$$\Delta\delta_{ht} = \frac{\omega\Delta C_p}{K} \tag{13}$$

As can be seen in Fig. 2 the step in phase angle is well related to the step in heat capacity at the glass transition. Sample b with about twice the mass of Sample a shows according to Eq. (13) about twice the step of Sample a in phase angle ($\Delta\delta_a \approx 0.01$ rad, $\Delta\delta_b \approx 0.025$ rad). The remaining difference may be due to some change of heat conductance inside the samples or between sample and pan.

To get information about the influence of thermal conductivity on the phase angle, samples of different contact area between sample and pan were prepared. Curve c in Fig. 2 shows the phase angle for a spherical shaped granulate. The observed phase angle is much more higher than that of the planar disk shaped samples and the step is more accentuated.

At temperatures above the glass transition often a decrease of the phase angle can be observed (e.g. Curve b). Because heat capacity is still increasing in this temperature region the only explanation for this behaviour is an increase of heat conductance. This may be caused by some changes in the contact area between sample and pan due to softening of the

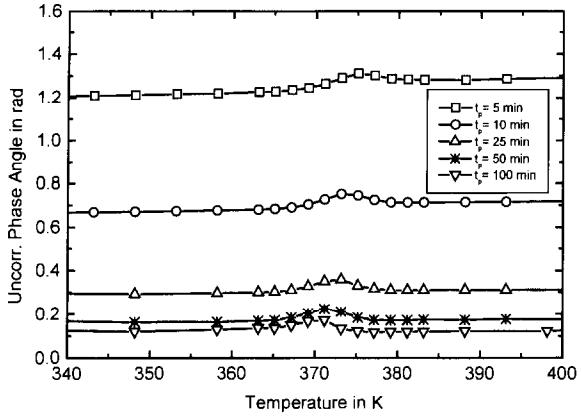

Fig. 4. Frequency dependence of uncorrected phase angle between heat-flow rate and heating rate for quasi-isothermal TMDSC measurements of polystyrene in the glass-transition region for different modulation periods. (Seteram DSC 121: m_{PS} = 230.44 mg; t_p =5–100 min; $q_0 = 0$; $T_a = 0.1$ K.)

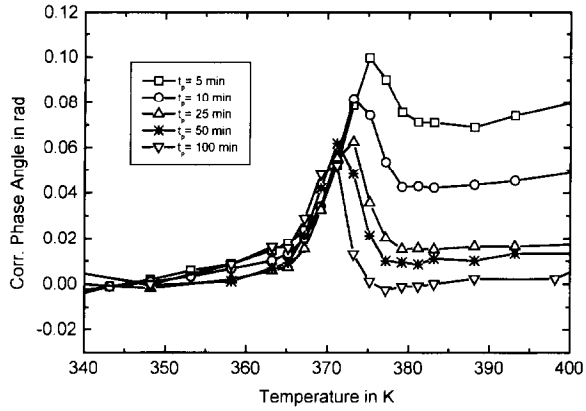

Fig. 5. Same as in Fig. 4 but for all curves the phase angle value at 350 K has been subtracted.

sample. To check this some silicon oil was added in between pan and sample to realise good and constant thermal contact. As expected the phase angle (see Curve d) is lowered compared to Curve b nevertheless it increases over the whole temperature range as the heat capacity does.

To demonstrate that the observed step change in the phase angle curve is not related to the underlying cooling the frequency dependence of the phase angle was studied in a quasi-isothermal experiment with the Setaram DSC-121. The results are shown in Fig. 4. As expected from Eq. (8), doubling the frequency yields double phase angle. In addition, with increasing frequency the step change in the phase angle becomes more and more pronounced as can be seen from Fig. 5 where the phase angle at about 350 K (see Fig. 4) has been subtracted. The observed shift in the maximum position reflects the shift of glass transition temperature with frequency. The opportunity for such heat capacity spectroscopy is one of the benefits of TMDSC [20–22]. To perform heat capacity spectroscopy in the glass-transition region and to compare the results with other measurements, for example, from 3ω method [23–25], a correct determination of complex heat capacity is necessary. With a thin disk shaped sample (Curve a in Fig. 2) or with low modulation frequencies it seems to be possible to perform measurements where the peak in phase angle is only little disturbed by effects due to heat transfer. Then a correction by subtraction of a straight line may be useful as a zero approximation for heat transfer part of the phase angle. It is not possible to realise optimal measuring conditions for all measurements in a wide frequency range, see Fig. 5. Therefore we are in need of a better correction than the subtraction of a straight line for the related heat transfer part of phase angle.

As demonstrated by the experiments, see Figs. 2 and 4, Eq. (8) is valid in the glass transition range of polymers. From this and from the a priori knowledge that the phase angle δ_s related to the relaxation process vanishes outside the relaxation region a better correction can be derived. For constant frequency and constant heat conductance the phase angle δ_{ht} is proportional to the sample heat capacity. Therefore we can scale a curve proportional to the measured heat capacity in such a way that it fits to the measured phase angle δ outside the glass-transition region. Subtracting this curve from the measured phase angle curve results in a better correction for the phase angle δ_{ht} given by Eq. (8) over the whole temperature range, see Fig. 6. The sample with oil is used to keep the thermal contact constant. At first the heat capacity modulus was changed by a linear relation ($\delta_{ht} \approx a + b|C_p^*(T)|$) in such a way that it fits to the measured phase angle at 340 and 400 K to determine the constants a and b. This fit is very well all over the curve outside the transition region for this sample. The difference $\delta - \delta_{ht}$ yields a corrected phase angle δ_s which is near to that of the thin disk.

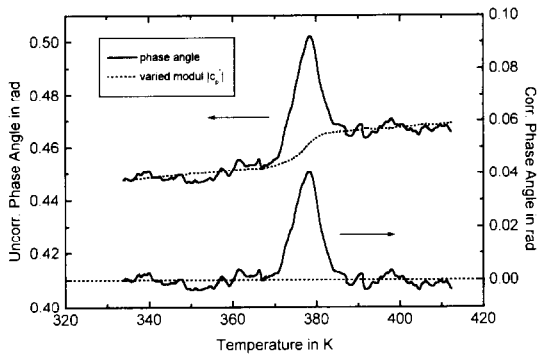

Fig. 6. Phase angle correction for the thick PS disk with some oil of a TMDSC measurement in the glass transition region, see text. (PE DDSC-7: m_{PS} = 27.23 mg; t_p = 1 min; q_0 = −0.5 K/min; T_a = 0.2 K.)

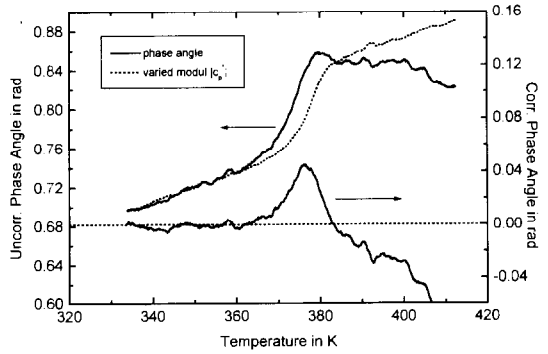

Fig. 7. Phase angle correction for PS-granulate of a TMDSC measurement in the glass transition region, see text. (PE DDSC-7: m_{PS} = 9.16 mg; t_p = 1 min; q_0 = −0.5 K/min; T_a = 0.2 K.)

A correction is much more difficult when thermal conductivity is changing during the measurement, see Fig. 7. In this case the modulus curve can only be fitted to the phase angle at low temperatures. The step height must be estimated from the step in the heat capacity according to Eq. (13). Heat conductance K can be calculated from phase angle at low temperatures according to Eq. (8). The correction needs, however, the knowledge of the part of the phase angle caused by heat transfer inside the oven and the pan (empty pan measurement correction). We are not able to perform such empty pan measurements because of the problems with the saw tooth modulation discussed above.

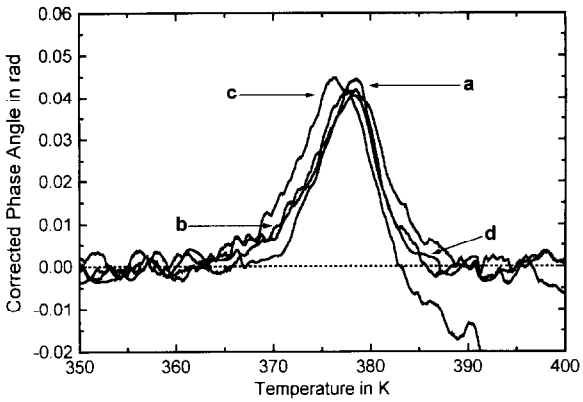

Fig. 8. Corrected phase angles between heat-flow rate and heating rate of TMDSC measurements of polystyrene in the glass transition region; a – thin disk, m_{PS} = 12.67 mg; b – thick disk, m_{PS} = 27.23 mg; c – granulate, m_{PS} = 9.16 mg; d – thick disk with silicon oil, m_{PS} = 27.23 mg. (PE DDSC-7: t_p = 1 min; q_0 = −0.5 K/min; T_a = 0.2 K.)

The uncertainty of the corrected phase angle in Fig. 7 is much more higher than that in Fig. 6 where thermal conductivity does not change during the measurement. The remaining decrease in phase angle of the corrected curve at high temperatures in Fig. 7 is an artefact due to the increase of thermal conductivity and has nothing to do with a change in complex heat capacity. At the moment we do not know any possibility to correct for such effects. As a result one has to be very careful when interpreting complex phase angle behaviour. The often reported negative phase angle values in the temperature range between glass transition and the onset of cold crystallisation of PET [21,22,26] may be caused by such changes in thermal conductivity and thus a wrong correction for the heat transfer related phase angle δ_{ht}.

To demonstrate the power of our correction method, in Fig. 8 corrected phase angles for all samples are plotted. Compared to the big differences of the measured phase angles, the differences of the corrected values are relatively small. From these corrected phase angles better real and imaginary parts of the complex heat capacity can be obtained according to Eqs. (11) and (12). The corresponding curve for the thin disk of PS is plotted in Fig. 9. The curve shape of $C_p''(T)$ corresponds well with the first derivative of $C_p'(T)$ as expected for amorphous samples and can be fitted with a Gauss function [27–29]. This Gauss fit gives the

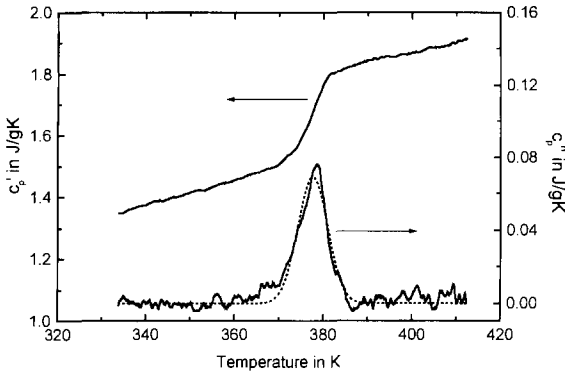

Fig. 9. Real (C_p') and imaginary part (C_p'') of complex heat capacity (C_p^*) for the thin disk of polystyrene. The dotted line describes a Gauss-fit with $T_0 = 377.6$ K and $\sigma = 3.3$ K. (PE DDSC-7: $t_p = 1$ min; $q_0 = -0.5$ K/min; $T_a = 0.2$ K.)

opportunity for direct comparison of curve shapes from 3ω method and TMDSC as described in [30].

5. Conclusion

From dielectric and mechanic dynamic measurements it is well known that the measured phase angle between electric field strength and current or stress and strain is direct related to sample properties like the imaginary part of the dielectric function or of the mechanical compliance, respectively. This is due to the fact that electric field and mechanical stress propagate in the sample much more faster than the modulation period. In the case of calorimetry we have to remember that heat does not propagate in the sample but has to flow into the sample. Heat flow needs temperature gradients and it is a time consuming process with time constants comparable with the modulation period. Therefore in TMDSC the measured phase angle is the superposition of an always appearing phase angle caused by heat transfer and perhaps a second one caused by relaxation processes within the sample. Only for measurements under optimal measuring conditions: thin sample with constant and high heat conductance between thermometer and sample as well as long modulation periods, the sample phase angle is only little disturbed by the heat transfer related phase angle.

The determination of frequency dependent complex heat capacity in the temperature region of a relaxation process, for example, glass transition, presupposes a correction for the part of the phase angle which is caused by heat flow. We suppose a correction taking into account the change of heat flow related phase angle due to the change in heat capacity. Our correction results in a phase angle which is nearly independent on the measuring conditions. Furthermore, the calculated complex heat capacities are in good agreement with those predicted by model calculations of Hutchinson [1] and Stoll [31]. This correction enables the determination of the complex heat capacity in a relatively wide frequency range, 10^{-4} to 0.1 Hz, with TMDSC equipment and to perform heat capacity spectroscopy. The respective results from glass transition in different glass forming substances will be presented in the future. A reasonable correction of phase angles is also necessary if one wants to compare measured complex heat capacities with those of model calculations or wants to study the influence of different sample treatment on complex heat capacity in the glass-transition region.

Acknowledgements

The authors gratefully acknowledge many interesting and clarifying discussions with G.W.H. Höhne, J. Hutchinson, J. Korus, S. Montserrat, J.E.K. Schawe, B. van Mele and B. Wunderlich.

References

[1] J.M. Hutchinson and S. Montserrat, this issue.
[2] B. Wunderlich, A. Boller, I. Okazaki and S. Kreitmeier, J. Thermal Anal., 47 (1996) 1013, 1026.
[3] P.S. Gill, S.R. Saurbrunn and M. Reading, J. Thermal. Anal., 40 (1993) 931, 939.
[4] M. Reading, Trends Polym. Sci., 8 (1993) 248, 253.
[5] M. Reading, B.K. Hahn and B.S. Crowe, US Patent 5,224,775 (06.07.93).
[6] J.E.K. Schawe, Thermochimica Acta, 260 (1995) 1, 16.
[7] B. Wunderlich, Y.M. Jin and A. Boller, Thermochim Acta, 238 (1994) 277, 293.
[8] J.E.K. Schawe, Thermochimica Acta, 261 (1995) 183, 194.
[9] E. Gmelin, this issue.
[10] P. Sullivan and G. Seidel, Ann. Acad. Sci. Fennicae A VI (1966) 58, 62.
[11] P.F. Sullivan and G. Seidel, Phys. Rev., 173 (1968) 679, 685.
[12] M. Castro and J.A. Puertolas, this issue.
[13] A. Hensel and C. Schick, this issue.

[14] I. Alig, this issue.
[15] Y.H. Jeong, this issue.
[16] J. Korus, M. Beiner, K. Busse, S. Kahle and E. Donth, this issue.
[17] J.E.K. Schawe, this issue.
[18] G.W.H. Höhne, H.K. Cammenga, W. Eysel, E. Gmelin and W. Hemminger, Thermochimica Acta, 160 (1990) 1.
[19] See textbooks of physics e.g.: C.J.F. Böttcher, and P. Bordewijk, Theory of Electric Polarisation, Elsevier, Amsterdam, 1978.
[20] A. Boller, C. Schick and B. Wunderlich, Thermochimica Acta, 266 (1995) 97, 111.
[21] A. Hensel, J. Dobbertin, J.E.K. Schawe, A. Boller and C. Schick, Journal of Thermal Analysis, 46 (1996) 935, 954.
[22] J.E.K. Schawe, Thermochimica Acta, 271 (1996) 127, 140.
[23] N.O. Birge and S.R. Nagel, Physical Review Letters, 54 (1985) 2674, 2677.
[24] N.O. Birge, Physical Review B-Condensed Matter, 34 (1986) 1631, 1642.
[25] N.O. Birge and S.R. Nagel, Review of Scientific Instruments, 58 (1987) 1464, 1470.
[26] J.E.K. Schawe and G.W.H. Höhne, Journal of Thermal Analysis, 46 (1996) 893, 903.
[27] E. Donth, Physica Status Solidi B, 74 (1976) K49, K52.
[28] D.J. Hourston, M. Song, A. Hammiche, H.M. Pollock and M. Reading, Polymer, 37 (1996) 243, 247.
[29] M. Song, A. Hammiche, H.M. Pollock, D.J. Hourston and M. Reading, Polymer, 36 (1995) 3313, 3316.
[30] S. Weyer, A. Hensel, J. Korus, E. Donth and C. Schick, this issue.
[31] B. Stoll, Private communication, 1996.